Stanford Exploration Project, Report 114, October 14, 2003, pages 71–81

Kinematics of 3-D angle-domain common-image gathers for migration velocity analysis

Thomas Tisserant and Biondo Biondi[1]

ABSTRACT

We extend the study of the kinematic properties of 2-D offset- and angle-domain common-image gathers to the general 3-D problem. We examine how the use of an incorrect migration velocity affects the behavior of the image in the offset and angle domains.
We show that the general 3-D case with and without the correct migration velocity can be cast into a 2-D formulation, making it possible to apply existing theory from 2-D. We illustrate both ray-tracing and plane-wave approaches to the problem and verify our theoretical results with a synthetic model.

INTRODUCTION

Migration Velocity Analysis (MVA) and Amplitude Versus Angle (AVA) analysis are the two main applications of Angle-Domain Common-Image Gathers (ADCIGs). ADCIGs can be computed in the Fourier domain from offset-domain images generated by wavefield-continuation methods (Sava and Fomel, 2000). In previous work (Tisserant and Biondi, 2003), we presented an extension of the method to make it valid for 3-D geometries. Biondi and Symes (2003) analyze the kinematics of ADCIGs when an incorrect migration velocity has been used during the wavefield-continuation step. This paper aims to extend their analysis to 3-D.

We consider two approaches: one based on rays, the other based on plane-waves. In the ray approach, we split our analysis between the use of an correct and an incorrect migration velocity. When the migration velocity is correct, the source and receiver rays focus at the same correct image point where they are coplanar. This property of the rays makes it simple to transform the 3-D geometry into 2-D for which the theory is available (Biondi and Symes, 2003). We then analyze the problem when an incorrect migration velocity is used. Incorrect migration velocity yields non focused ray resulting in an apparent image point, and generally not coplanar rays. We introduce an apparent propagation plane in which the 2-D theory can be applied. We will then discuss a plane-wave approach of the problem. Finally a synthetic example is used to verify our theoretical results.

[1]**email:** thomas@sep.stanford.edu, biondo@sep.stanford.edu

GEOMETRY

Extension from 2-D to 3-D requires the introduction of new angles in the geometric definition of the problem. However, we will see that a 3-D problem can be formulated as a 2-D problem whose analysis is done by Biondi and Symes (2003).

In 2-D, two angles define the geometry of the problem: the dip of the interface, α, and the aperture of the reflection, γ. In 3-D, the reflector is not only defined by its dip α, but also by its azimuth ϕ. Further, in the full 3-D geometry, the rays are not necessarily coplanar during downward-continuation. As a consequence, the reflection may have a different azimuth than the azimuth of the survey. We call β the reflection azimuth. When the correct migration velocity is used, the two rays focus correctly in one point. Near this image point the two rays define defines one plane. The most general configuration considers an incorrect migration velocity. Because the velocity is incorrect, the rays do not focus in one point. Instead, they stop as two different points with the same depth when using downward continuation. The distance between the two points is the offset at constant z. The middle of the segment is the image point in the offset domain domain at constant z (zODCIG). In such configuration, the rays are not necessarily coplanar. We introduce a new angle, ξ, accounting for the non-coplanarity of the rays. To make the link with the 2-D case, we seek an apparent propagation plane containing all the information about the actual geometry. In all cases, the image point in the angle domain moves along the normal to the apparent interface by an amount dependent on the migration velocity used, and on the aperture angle. The image point in the angle domain is obtained by transforming of the image point in the offset-domain. We use the post-migration transformation in the Fourier domain introduced in Sava and Fomel (2000) for the 2-D geometry, and its 3-D extensions by Tisserant and Biondi (2003) for the 3-D full prestack migration. Our approach in the next two sections is based on a ray construction. Later, we will present in the third section another approach based on plane-waves.

CORRECT MIGRATION VELOCITY

Discussion

The 3-D geometry implies that the rays can now have different azimuth and can propagate out of the vertical plane. If the migration velocity is correct, the two rays focus at the same point at zero subsurface offset (Figure 1). By assuming the velocity is constant around the image point, all the elements (rays, normal, image points) are contained in one plane: the plane of the propagation. By an appropriate change of coordinates, this 3-D problem with correct migration velocity can be locally transformed in a 2-D problem, and the 2-D theory analyzed by Biondi and Symes (2003) be applied. The offset-to-angle transformation must be adapted though.

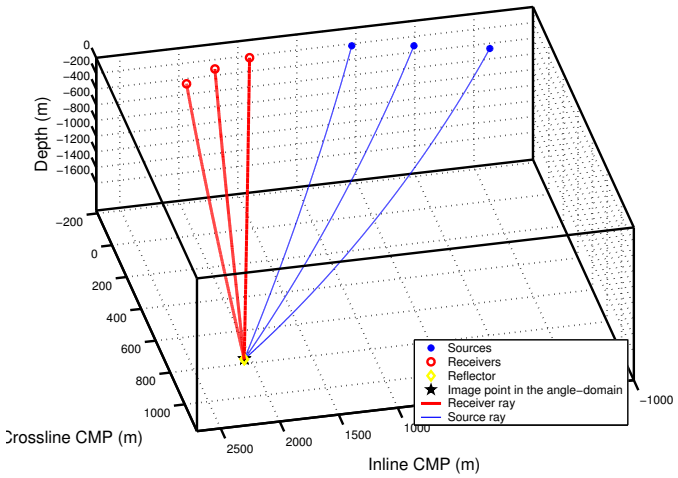

Figure 1: The velocity function is $V(z) = 1.5 + .5z$ km/s. The target has a fixed position, azimuth ($\phi = 45$) and dip ($\alpha = 60$). thomas1-multi_correct_v_2 [CR]

Offset-to-angle transformation

In 2-D, the offset-to-angle transformation is done with the relation

$$\tan\gamma = -\frac{k_h}{k_z}, \tag{1}$$

where γ is the aperture angle of the reflection, k_h is the offset wavenumber associated with the subsurface horizontal offset, and k_z is the vertical wavenumber. Tisserant and Biondi (2003) presented a 3-D generalization of Equation 1:

$$\tan\gamma = -\frac{k'_{h_x}}{\sqrt{k_z^2 + k'^2_{m_y}}}, \tag{2}$$

$$k'_{h_y} = -\frac{k'_{m_y} k'_{m_x} k'_{h_x}}{k_z^2 + k'^2_{m_y}} \tag{3}$$

where $\mathbf{k}_m$ and $\mathbf{k}$_h are the midpoint and offset vector wavenumber, respectively, and where the reflection azimuth, β, is introduced through

$$k'_{m_x} = \cos\beta k_{m_x} - \sin\beta k_{m_y} \tag{4}$$

$$k'_{m_y} = \cos\beta k_{m_x} + \sin\beta k_{m_y} \tag{5}$$

$$k'_{h_x} = \cos\beta k_{h_x} - \sin\beta k_{h_y} \tag{6}$$

$$k'_{h_y} = \cos\beta k_{h_x} + \sin\beta k_{h_y}. \tag{7}$$

The offset-to-angle transforms a $(k_z, k_{m_x}, k_{m_y}, k_{h_x}, k_{h_y})$ five dimensions cube into another 5-D one $(k_z, k_{m_x}, k_{m_y}, \gamma, \delta)$. Figure 2 is the measured aperture-azimuth distribution for the configuration displayed in Figure 1 obtained with ray-tracing. We set the lower boundary in γ because of an increased incertitude in the estimation of β as γ gets close to 0. The upper boundary in γ is reached when one of the two rays begins to overturn.

We now present a more complex 3-D extension: the one addressing the 3-D full prestack migration with a wrong migration velocity.

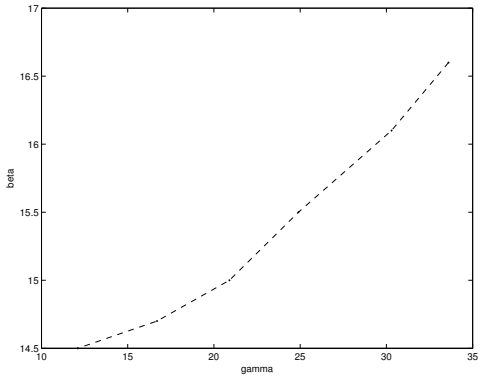

Figure 2: $\gamma - \beta$ distribution corresponding to Figure 1 thomas1-beta_f_gamma_v_correct [NR]

INCORRECT MIGRATION VELOCITY

Discussion

Figure 3 presents the geometry of the problem throughout an example. It has been built con-

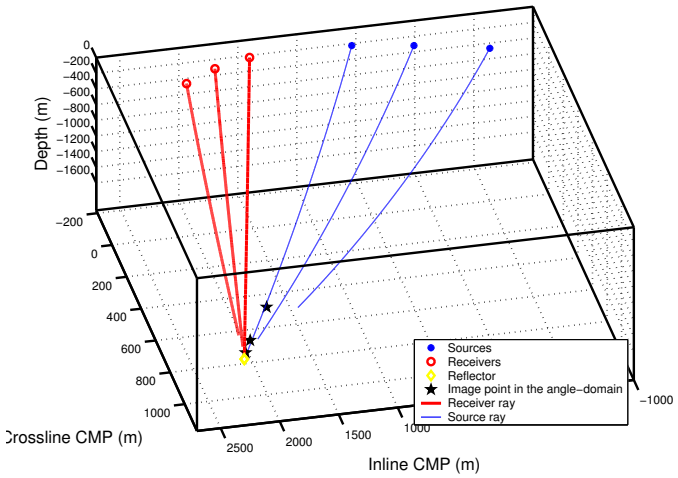

Figure 3: Ray-tracing with the incorrect velocity function $V(z) = 1.41 + .47z$ km/s. Because the velocity is too slow, the rays end at too shallow of a depth. thomas1-multi_incorrect_v_2 [CR]

sidering the same events as in Figure 1 but by using an incorrect velocity. Because the velocity is too low, the rays stop at too shallow of a depth, where they are not coplanar. The gap between the source and the receiver endpoints is the horizontal offset (zODCIG, z for constant z). The middle of the horizontal offset is the image point in the zODCIG domain. One can measure on Figure 3 the azimuth of the source-receiver end points segment. We call it β'. β' can be decomposed into two components: one, β, is the azimuth due to ray-bending, the other, ξ, accounts for the non-coplanarity due to the use of an incorrect migration velocity. If the migration velocity is too slow, the rays stop too early, yielding to an underestimated reflection azimuth. Conversely, if the migration velocity is too high, the rays stop too late, yielding to a overestimated reflection azimuth. When the velocity is exact, the rays are coplanar and the rotation of the reflection azimuth is only due to ray-bending and dips.

ODCIGs and ADCIGs properties

The velocity is assumed to be constant in a small volume around the image points. That is why the rays are straight lines in the next few pictures.

Biondi and Symes (2003) noted that, in 2-D, image points in the offset domains (at constant x, xODCIG, and constant z, zODCIG) lie on an apparent interface. In 2-D the apparent interface is a line, whereas it is a plane in 3-D. Not only the image points belong to the interface, but they are also all collinear (Figure 4). From this property we can define a new plane that includes the normal and the common line of the image points in the offset domains. This plane has special properties since it contains all the image points: it is the link to the 2-D case. Let us further study this plane.

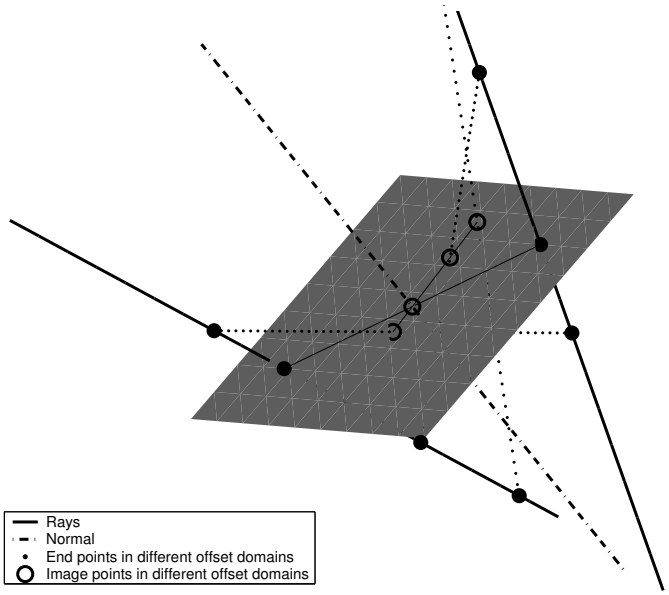

Figure 4: The endpoints and image points of all the offset-domain gathers are displayed (dotted lines). All the image points are defined in the interface and are collinear. thomas1-OCIGs_alignment [CR]

If the velocity is incorrect, the rays do not focus at the actual image point but at an apparent image point located in the middle of the end points of the two rays. The apparent image point is the image point in the offset domain. Further, in the case of full prestack migration, the rays are not coplanar, so there is no propagation plane. Physics requires one though. In the absence of a propagation plane, we define an apparent propagation plane. To find it, we start from the actual rays and find a rotation that makes their image coplanar. The rotation is done around the normal at the interface (Figure 5). Note that the new rays are parallel to the original ones but have different end points. The plane in which the rays are coplanar after rotation is the apparent propagation plane. The geometric location of the image points in the offset-domain is at the intersection between the propagation plane and the interface. The rotated rays thus define the same plane-wave as the original rays. The angle of the rotation, ξ, is equal to the azimuth defined in the interface of both source and receiver rays. The reflection azimuth, β, is equal to the azimuth of the apparent propagation plane.

We now analyze how the image in the angle domain is obtained from the image in the offset domain.

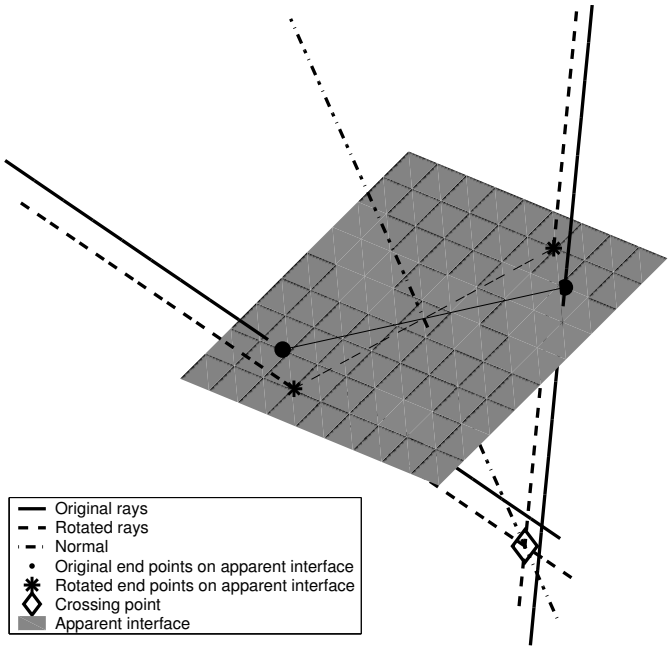

Figure 5: Transformation of the original rays into coplanar rays. The source an receiver endpoints (the 2 big dots) are rotated around the normal until the rays are coplanar. Note that the new rays and azimuth of the rays measured in the apparent interface. the normal cross at the same point. The two new rays and the normal define the apparent propagation plane. thomas1-rot_copl [CR]

Offset-to-angle transformation.

The apparent propagation plane plays another interesting role during the offset-to-angle transformation: despite the non-coplanarity of the rays, the energy moves only in the apparent propagation plane. Figure 6 illustrates this property. Two offset-domain image points are displayed. points in the offset domain to the image point in the angle domain along a direction orthogonal to the direction of the offset. All the possible directions define a plane. The two orthogonal planes are displayed on Figure 6. The intersection of the two planes with the normal gives the position of the image point in the angle domain. More specifically, the energy moves at the intersection between the orthogonal plane and the apparent propagation plane. To sum up, when an incorrect migration velocity is used, the rays are not coplanar. There is however a preferential plane, the apparent propagation plane, which allows one to cast the 3-D problem into a 2-D one.

PLANE-WAVE APPROACH

In the previous sections, we have talked about rays or ray-tracing. This approach has the advantage of being intuitive. The physics, however is governed by plane-waves. In this section we present a plane-wave approach of the same problem.

Why plane-waves

One reason to use plane-waves instead of rays is to avoid the asymptotic approximation introduced when using rays. Unlike rays, each plane-wave can be treated independently at each

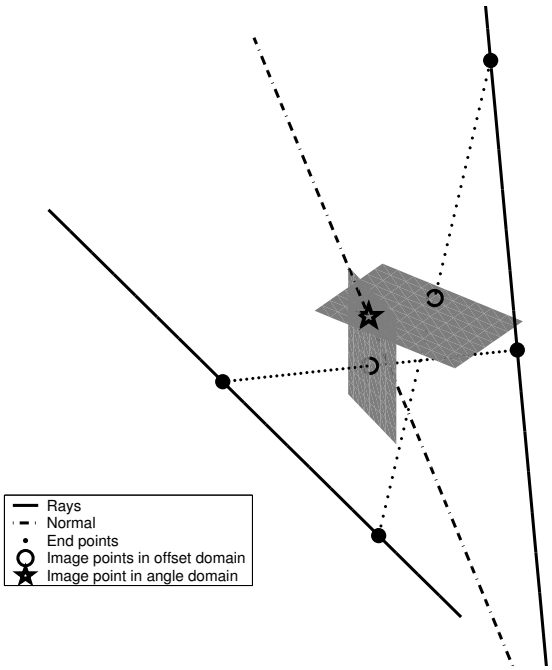

Figure 6: Geometric construction of the image point in the angle domain from the image points in the offset domain. thomas1-gamma_planes_2 [CR]

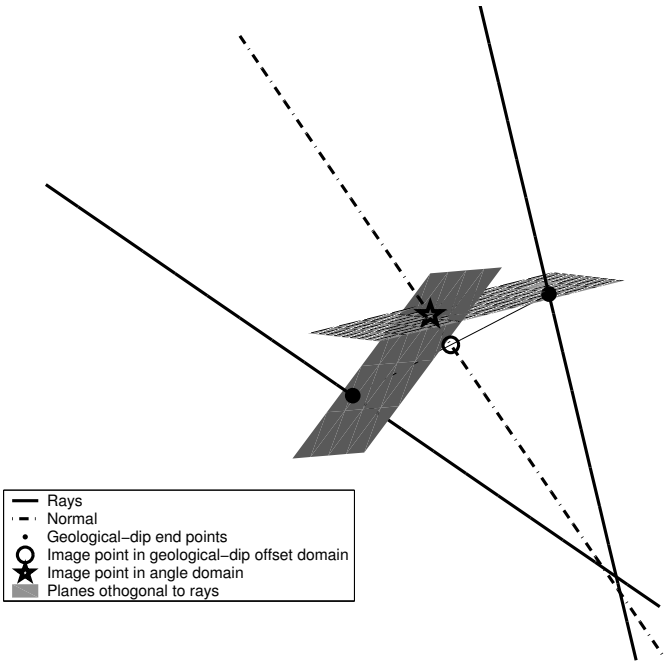

Figure 7: Geometric construction of the image point in the angle domain from the source and receiver rays end points. thomas1-gamma_planes [CR]

frequency. The use of plane-waves simply ignores the problem of non-coplanar rays. Indeed, the original and the rotated rays described earlier share the same plane-wave. The reflection azimuth is the azimuth of the apparent propagation plane which is directly deduced from the angles of the two plane-waves.

Construction

Given one image point in the angle domain, and the four angles defining the two plane-waves (two azimuths and two dips), the two plane-waves are positioned such that the image point is contained in both. The directions of the two plane-waves provide the azimuth and the dip of the reflector. The image point is contained in the intersection of the two plane waves. To find the plane of the reflection we define the apparent propagation plane as being orthogonal to the two plane-waves and passing through the image point. Once this plane defined, knowledge of the rays location and coplanarity is inconsequential.

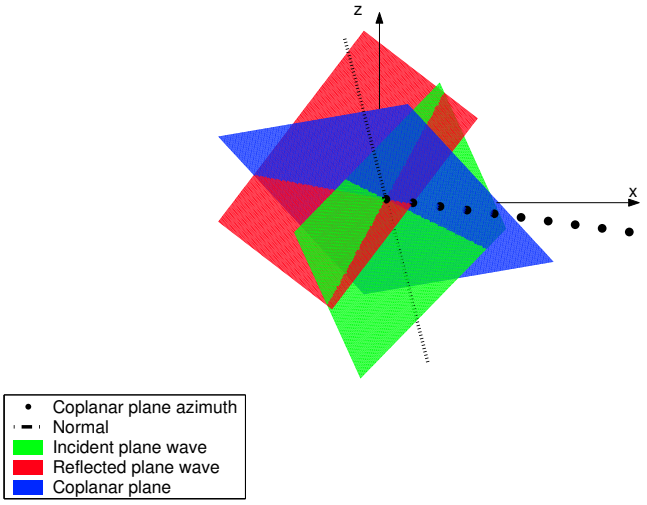

Figure 8: Plane-wave construction. thomas1-plane_waves [NR]

SYNTHETIC EXAMPLE

We verify our theoretical results on a model with five slanted planes (Vaillant and Biondi, 2000). The velocity function is $v(z) = 1.5 + .5z$ km/s. The velocity gradient allows us to highlight the rotation of the reflection azimuth due to ray-bending. The model consists of five planes with 0°, 15°, 30°, 45°, 60° dip and a 45° azimuth. The dataset is migrated with full prestack migration. We migrate first with the correct velocity and then with a velocity that is 6% too slow. The migrated model is then transformed from offset to angle for different reflection azimuths. Hence the image has five dimensions: in-line and cross-line midpoints, depth, aperture and reflection azimuth. We select one midpoint and obtain a cube of a midpoint gather sorted in aperture angle and reflection azimuth angle.

Behavior of the reflection azimuth

Figure 9 shows one depth slice in the (z, γ, β) cube at $z = 1450\ m$. We observe that the reflection azimuth changes slowly with the aperture angle, except at small angles where the uncertainty is high. This slow variation is consistent with Figure 2 since the reflection azimuth changes by 2° while the aperture changes by 25°. One can also notice that the maximum aperture angle obtained with ray-tracing, 35°, is consistent with the aperture angle interval where the energy is high. The reason may be that rays begin to overturn when the aperture angle is higher than 35°. Indeed, the upper limit in ray-tracing is due to one of the ray beginning to overturn.

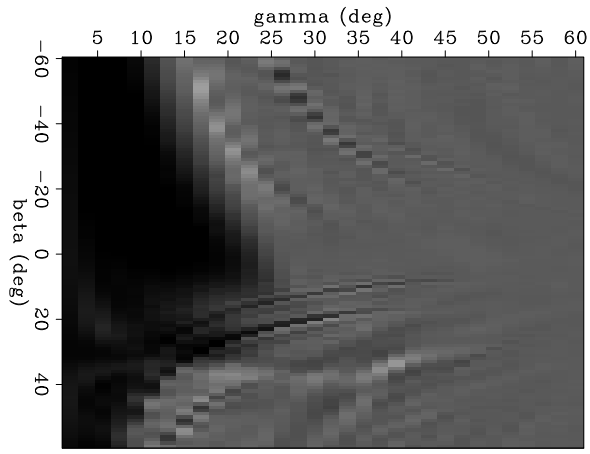

Figure 9: Depth slice in the (z, γ, β) cube. thomas1-2d_v_1 [CR]

ADCIGs movement with wrong velocity

We use the ray-tracing to predict the localization of the energy in the synthetic dataset migrated with the wrong velocity. The ray-tracing is illustrated by Figure 3. Starting from the true position of the image point (the diamond on the Figure), we seek the position of the image point (stars on the figure) when an incorrect migration velocity is used. The reflector has a fixed azimuth and dip. We first model the events recorded at the surface at one particular aperture and reflection azimuth. Once the true events are known, the source and the receiver rays are shot in a media with an incorrect velocity this time. If the velocity is too slow, then the rays stop at two distinct end points. Knowing the position of the end points and the ray parameters, the position of the image point in the angle domain for an incorrect migration velocity is determined through a geometric construction similar to the one in 6. It is also possible to use the normal shift described in the 2-D case since we have shown that the 3-D problem can be recast as 2-D one. We test this procedure on an image point on the 60° dip reflector and whose location is $(400, 400, 1300)$ in image. We choose a source-receiver pair such as the aperture angle is 32°. Again, our goal is to find where the true image point has moved because of the use of an incorrect migration velocity. We observe on Figure 10 that the coordinates of the apparent image point in the angle domain computed by ray-tracing do match those of the image point in the model migrated with the wrong velocity.

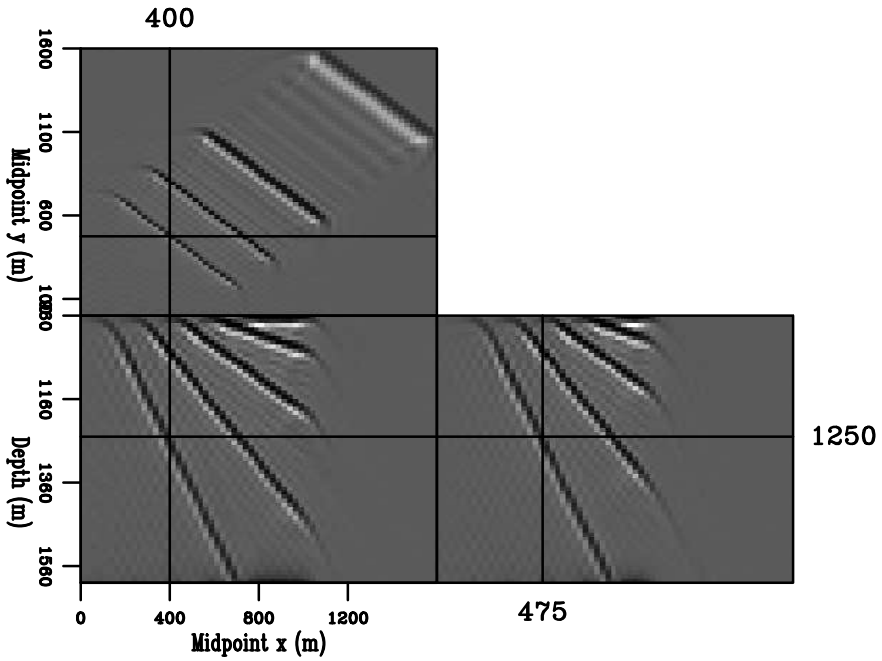

Figure 10: Dataset migrated with the incorrect velocity. thomas1-cube_0_I0 [CR]

CONCLUSIONS

We have presented a 3-D study of the kinematic of angle-domain common-image gather. Knowing the theory in 2-D, we showed how a 3-D configuration can be casted in a 2-D formulation. The transition is straightforward when a correct velocity is used since the plane of the propagation is the plane in which the problem becomes 2-D. In the less obvious problem where an incorrect migration velocity is used, we have defined an apparent propagation plane that fulfills the same objective. We have presented both a ray-based and a plane-wave approach. The kinematic observations made with ray-tracing have been verified on a synthetic dataset.

REFERENCES

Biondi, B., and Symes, W., 2003, Angle-domain common-image gathers for migration velocity analysis by wavefield-continuation imaging: SEP–**113**, 177–210.

Sava, P., and Fomel, S., 2000, Angle-gathers by Fourier Transform: SEP–**103**, 119–130.

Tisserant, T., and Biondi, B., 2003, Wavefield-continuation angle-domain common-image gathers in 3-D: SEP–**113**, 211–220.

Vaillant, L., and Biondi, B., 2000, Accuracy of common-azimuth migration approximations: SEP–**103**, 157–168.